Check for updates

Received: 9 August 2020 | Accepted: 4 May 2021

DOI: 10.1113/EP089000

Experimental Physiology WILEY

RESEARCH PAPER

STZ-diabetic rat heart maintains developed tension amplitude by increasing sarcomere length and crossbridge density

Raffaella Isola[1] | Francesca Broccia[2] | Alberto Casti[1] | Francesco Loy[1] | Michela Isola[1] | Romina Vargiu[2]

[1] Department of Biomedical Sciences, Division of Cytomorphology, University of Cagliari, Cittadella Universitaria di Monserrato, SP 8, Monserrato, Italy

[2] Department of Biomedical Sciences, Division of Physiology, University of Cagliari, Cittadella Universitaria di Monserrato, SP 8, Monserrato, Italy

Correspondence
Romina Vargiu, Department of Biomedical Sciences, Division of Physiology, University of Cagliari, Cittadella Universitaria di Monserrato, SP 8, 09042 Monserrato, Italy.
Email: rvargiu@unica.it

Funding information
Sardinian Region Government, Grant/Award Numbers: 7/2007, CRP 366 60052

Edited by: Michael Tipton

Abstract

We investigated whether diabetes-associated altered ventricular function, in a type I diabetes animal model, results from a modification of acto-myosin interactions, through the *in vitro* recording of left papillary muscle mechanical parameters and examination of sarcomere morphology by transmission electron microscopy (TEM). Experiments were performed on streptozotocin-induced diabetic and age-matched control female Wistar rats. Mechanical isometric and isotonic indexes and timing parameters were determined. Using Huxley's equations, we calculated mechanics, kinetics and energetics of myosin crossbridges. Sarcomere length and A-band length were measured on TEM images. Type I and III collagen and β-myosin heavy chain (MHC) expression were determined by immunoblotting. No variation in resting and developed tension or maximum extent of shortening was evident between groups, but diabetic rats showed lower maximum shortening velocity and prolonged timing parameters. Compared to controls, diabetics also displayed a higher number of crossbridges with lower unitary force. Moreover, no change in type I and III collagen was associated to diabetes, but pathological rats showed a two-fold enhancement of β-MHC content and longer sarcomeres and A-band, detected by ultrastructural morphometry. Overall, these data address whether a preserved systolic function accompanied by an altered diastolic phase results from a recruitment of super-relaxed myosin heads or the phosphorylation of the regulatory light chain site in myosin. Although the early signs of diabetic cardiomyopathy were well expressed, the striking finding of our study was that, in diabetics, sarcomere modification may be a possible compensatory mechanism that preserves systolic function.

KEYWORDS
crossbridges, myocardial contractility, streptozotocin-induced diabetes

1 | INTRODUCTION

Diabetes mellitus (DM) is one of the major concerns of public health as it affects about 300 million people worldwide and its incidence is constantly increasing. The International Diabetes Federation has estimated that there will be about 552 million people with diabetes (type I and II) by 2030 (Guariguata et al., 2014). Several studies have established DM as a potent and prevalent risk factor for

This is an open access article under the terms of the Creative Commons Attribution-NonCommercial License, which permits use, distribution and reproduction in any medium, provided the original work is properly cited and is not used for commercial purposes.
© 2021 The Authors. *Experimental Physiology* published by John Wiley & Sons Ltd on behalf of The Physiological Society

cardiovascular morbidity and mortality (Lee et al., 2015), since it is frequently associated with a specific cardiomyopathy, involving left ventricular dysfunction even in the absence of atherosclerotic coronary artery disease, hypertension or valvular disease. Recently, several studies reported that heart failure with preserved ejection fraction is the most frequent cardiomyopathy linked to type I diabetes. It usually incurs an 8–12% annual mortality rate (Henning, 2020; Huynet al., 2019; Takeda et al., 2011).

Usually, the most evident mechanical defect of type I diabetic cardiomyopathy is the impairment of left ventricular diastolic function, while the systolic function is conserved (Basu et al., 2009) or even enhanced (Heerebeek et al., 2008). In diabetic animal models, diastolic and systolic dysfunctions sometimes have been associated with a prolonged duration of contraction and relaxation, reduced velocity of contraction and relaxation, and depressed myocardial contractility in whole heart tissue, isolated ventricular myocytes (Fein et al., 1980; Ren & Bode, 2000; Waddingham et al., 2015) and isolated papillary muscles (Joseph et al., 2005).

The mechanisms that lead to the development of the diabetic cardiomyopathy are poorly understood, albeit several studies have aimed at clarifying them. The increased risk of cardiac dysfunction and other heart complications is mainly linked to hyperglycaemia and oxidant damage. Several mechanisms have been proposed regarding disease progression, including reduced energy production, accumulation of free radical species, myocardial fibrosis and the malfunction of intracellular calcium regulatory proteins (Fein & Sonnenblick, 1994; Hattori et al., 2000; Norby et al., 2004). Hence, chronic DM has been associated with impaired cardiac contractility and relaxation due to altered Ca^{2+} homeostasis (Lacombe et al., 2007; Trost et al., 2002). Numerous investigations reported decreased expression of sarcoplasmic reticulum Ca^{2+}-ATPase (SERCA) in diabetic rat hearts (Lacombe et al., 2007; Trost et al., 2002; Zhang et al., 2008; Zhao et al., 2014), leading to a cytosolic calcium overload during the diastolic phase due to a slower rate of calcium sequestration (Lacombe et al., 2007).

The underlying basis of diastolic cardiac disease could also be found in changes at the subcellular level of cardiomyocytes (Dhalla et al., 1998). Myocyte contractility is affected by qualitative and quantitative variations in contractile and regulatory proteins in STZ-induced diabetic rats (Kita et al., 1991; Malhotra & Sanghi, 1997). In several animal models of DM, the shift in myosin heavy chain (MHC) from α to β isoform, a reduced myofibrillar ATPase activity and a diminished calcium sensitivity of myofilaments are known to play a significant role in contraction and relaxation abnormalities (Dillmann, 1980; Dhalla et al., 1998; Kita et al., 1991; Malhotra & Sanghi, 1997). Morphological analysis has revealed loss and probable alteration of actin filaments (Nemoto et al., 2006; Thompson, 1994; Zhang et al., 2008), reduced myocyte diameter and increased extracellular matrix content in STZ-induced diabetic hearts (Ares-Carrasco et al., 2009; Asbun & Villarreal, 2006). All these data suggest that, in addition to subcellular modifications in the cardiomyocyte, alterations in sarcomeric proteins and/or connective tissue density may also contribute to diabetic cardiomyopathy development.

New Findings

- **What is the central question of this study?**
  In the papillary muscle from type I diabetic rats, does diabetes-associated altered ventricular function result from changes of acto-myosin interactions and are these modifications attributable to a possible sarcomere rearrangement?
- **What is the main finding and its importance?**
  For the first time, we showed that type-I diabetes altered sarcomeric ultrastructure, as seen by transmission electron microscopy, consistent with physiological parameters. The diabetic condition induced slower timing parameters, which is compatible with a diastolic dysfunction. At the sarcomeric level, augmented β-myosin heavy chain content and increased sarcomere length and cross-bridges' number preserve myocardial stroke and could concur to maintain the ejection fraction.

In all muscles including myocardium, the molecular motor mechanism that regulates the contractile properties depends on the number of active crossbridges, which singularly behave as independent force generators. In the present study, we hypothesized that the cardiac contractility dysfunctions induced by type-I diabetes could be also related to a modification of sarcomeres, in terms of interactions of their associated proteins. This hypothesis is supported by a study (Mancinelli et al., 2005) which highlighted changes in sarcomere length in response to severe cardiomypathy. The authors observed that impairment of the mechanisms that govern the mechanical functioning of cardiac pump was associated to an abnormally wide range of sarcomere length (shorter and longer) in a BIO T0-2 cardiomyopathic Syrian hamster animal model with dilated cardiomyopathy.

The qualitative and quantitative changes in acto-myosin interactions were investigated by measuring mechanical parameters, namely the developed tension and shortening velocity, and by calculating the total number, unitary force, kinetics and energetics of crossbridges in female diabetic rats, using Huxley's mathematical model. Since the active number of crossbridges also depends on the sarcomere length, we determined whether such differences could be ascribed to possible sarcomere modifications such as a change in the number and total sarcomere length, in a A-band length and β-MHC expression. As in diabetic cardiomyopathy, contractility dysfunction has also been ascribed to an abnormal extracellular matrix deposition, we evaluated whether in diabetes myocardial content of collagen I and III varied.

For the first time, we show that type-I diabetes altered sarcomeric ultrastructure, as seen by transmission electron microscopy, consistent with physiological parameters. The diabetic condition induced slower

timing parameters, which is consistent with diastolic dysfunction. Indeed, in our animal model diabetes induced prolongation of twitch duration, longer sarcomeres and increased number of crossbridges in cardiomyocytes, which might explain the observed unaltered developed tension found in diabetics.

2 | METHODS

2.1 | Ethical approval

This study was approved by the Committee on Animal Use and Care of University of Cagliari in accordance with the Italian Guidelines for the use of laboratory animals, which conform with the guidelines for care and use of experimental animals issued by the Italian Ministry of Health (D.L. 116/92) and by the EU Directive (2010/63/EU) and the *Guide for Care and Use of Laboratory Animals*, adopted by the NIH, USA (8th edition, 2011). Furthermore, it follows the principles and regulations of animal care, as described in the editorial by Grundy (2015). Moreover, according to D.L. 116/92 (Italian law for animal care), valid at the time of experimentation, after local ethical committee approval (N. 05/2013), the planned animal experimentation was sent for silent assent to the Italian Ministry of Scientific research and to all the legally responsible and veterinary organizations (opec271.20130730103706.30120.05.1.16@pec.aruba.it).

2.2 | Animals treatment

Fifty female Wistar Han rats, purchased from Harlan Laboratories (Indianapolis, IN, USA), initially weighing about 230 g and being about 10 weeks old, were used in this study. The animals were housed five per cage in a light–dark cycle of 12 h, temperature 22–24°C and 40–50% humidity, and received a standard diet (Mucedola s.r.l., Settimo Milanese, MI, Italy) and water *ad libitum*.

DM was induced by a single dose of streptozotocin (STZ) of 65 mg kg^{-1} i.p. dissolved in sodium citrate buffer pH 4.5 ($n = 30$). Age-matched controls ($n = 20$) were injected with vehicle only. The occurrence of diabetes was checked about 1 week after the injection and then monthly until the day of the experiment. Blood glucose content, ketone bodies and body weights were also tested monthly during the diabetic period (almost 5 months). The first two parameters were checked by means of specific stripes used on an Optium Xceed™ meter, Verio Flex (Life Scan). Blood was collected as follows: a drop was collected from the tip of the tail of each rat, by means of a small cut, which was disinfected right away. Sampling was performed monthly, so we reduced to the least all possible distress for the animals. After sufficient conditioning time, one animal was excluded from the experimental protocol for failure to reach a hyperglycaemic state.

2.3 | Papillary muscle preparation

After 19–20 weeks of DM, animals were killed by decapitation in a stress-free environment. This method of killing is included in Annex IV of EU Directive (2010/63/EU), when another method cannot be applied. Unfortunately, we could not use any drug to obtain the same effect, since that would be deleterious for the assessment of contractility of papillary muscle. The hearts were then quickly removed, and immersed in modified, oxygenated Krebs–Hanseleit solution at room temperature (24°C). Using a stereomicroscope, the left ventricle was opened, and the papillary muscles were dissected free. Functional experiments and ultrastructural studies were carried out on posterior and anterior papillary muscle, respectively.

The functional experimental set-up has been described previously (Eisenberg et al., 1980; Palmiter et al., 1999; Vargiu et al., 2010). The upper and lower ends of the left ventricular papillary muscle (PM) were tied between two small metal rings and vertically suspended in a 15 ml organ bath containing modified Krebs–Hanseleit solution with the following composition (in mM): NaCl 123, KCl 6.0, $CaCl_2$ 2.50, $MgSO_4$ 1.2, $NaHCO_3$ 20, KH_2PO_4 1.2, and glucose 11. The bath was vigorously aerated (Paradise et al., 1981) with an O_2 (95%)–CO_2 (5%) mixture that maintained a pH of 7.4 at a temperature of 32°C. For the isometric and isotonic studies, the metallic ring on the upper tendinous end of the muscle was attached to a force transducer (Mod.Wp1 Fort 10, 2200 μV/V/g, ADInstrument, Bella Vista, NSW, Australia) mounted on a rack and pinion enabling the muscle to be stretched to any desired length and held there isometrically. The lower ring was fastened to the lever of a linear displacement transducer (moment of inertia 35 g cm^{-2}, breakaway torque <0.1 g cm^{-2}, Basile, Comerio, Italy). Lever arm loading was provided by a tungsten alloy cylinder counterweight moving along a scale producing a load variation of 0.01 g/step. Two stops allowed the muscle to operate under isometric or isotonic conditions and to receive both preload and afterload. After an equilibration period of 1 h under a preload of 20 mN, the left ventricular PM was stimulated supramaximally via platinum plate electrodes, placed parallel to the muscle. Electrical stimulation was effected from a constant-current source (Multiplexing Pulse Booster, Basile) at the optimal force–frequency response for PM, that is, at a frequency of 0.06 Hz and with a stimulus duration of 5 ms. The electrical current intensity was set 10% higher than the minimum necessary to produce mechanical response (80–100 mA). Force and length data were sampled at a rate of 1 kHz and stored on disk for later analysis. Experimental data were analysed by the software Chart V.7.0 equipped with an analog-to-digital converter program (PowerLab, ADInstruments).

Two signals, force and shortening, were recorded under isometric or isotonic conditions in control and diabetic PMs. Under isometric conditions, stimulus–responses and length–tension studies were carried out to determine the L_{max}. L_{max} corresponded to the resting length at which the maximum isometric active developed tension was measured. All the experiments were performed at L_{max}. Under isotonic conditions, both force and shortening signals were simultaneously recorded at preload, corresponding to the passive tension recorded at L_{max}, and at various afterloads from preload until the isometric condition was reached. At the end of the experiments, cross-sectional area (CSA, in mm^2) was calculated from the ratio of fresh PM weight to L_{max}, assuming the geometry of a cylinder and a muscle density of 1.056.

2.4 | Papillary muscle mechanical parameters

Under isometric conditions, the following mechanical parameters were measured: resting tension (RT), i.e., the passive tension recorded at L_{max}; maximum developed tension (DT), i.e., the active tension recorded at L_{max}, corresponding to peak isometric tension; latency, the time measured from the stimulus artifact to the onset of the muscle contraction wave (excitation–contraction coupling); time to peak tension (TPT), the time from the onset of contraction wave to peak tension; half-time of relaxation (T½R), the time required for the force to fall from its maximum value to half that value; and peak rate of tension rise (+T′) and peak rate of tension fall (−T′), representing, for the full isometric contraction, the positive peak rate of the isometric tension derivative and the peak rate of tension decline, respectively. Alternatively, under isotonic conditions direct measurements of shortening at preload and at various afterloads were recorded from control and diabetic PMs. DT was normalized per CSA to obtain peak isometric tension (P_0; mN mm^{-2}), as well as RT (mN mm^{-2}), + T′ (mN s^{-1} mm^{-2}) and − T′ (mN s^{-1} mm^{-2}). The maximum extent of shortening recorded at preload (ΔL), was expressed as a percentage of L_{max} (L/L_{max}).

2.4.1 | Force–frequency relationship

The force–frequency relationship (FFR) was established on each PM by stimulating the muscle to contract at increasing frequencies: 0.06, 0.12, 0.25, 0.5, 1 and 2 Hz. To avoid excessive increase in resting tension, the maximum pacing frequency was set at 2 Hz. This frequency approximates the intrinsic rate of the isolated rat heart at 32°C (Han et al., 2014). The PMs were stimulated for ∼1–3 min to reach a steady state at each given frequency. Data were collected when the developed force remained consistent. FFR was evaluated at L_{max}. To avoid history or rundown effects that may occur in a stepwise protocol, the different frequencies were tested in a random order. For each tested frequency, the values of developed tension and timing parameters (TPT, T½R, +T′, −T′) of the last five contraction waves were averaged.

2.4.2 | Force–velocity response

The force–velocity relation was accurately fitted by hyperbola; the correlation coefficient between experimental data and points calculated from the hyperbolic curve had a high value ($r \geq 0.95$), indicating that Hill's equation provided a good fit. The force–velocity relation was established from the peak shortening velocity (V) plotted against the peak isotonic tension normalized per CSA (P) and measured contractions in which afterloads were progressively increased from zero up to the peak isometric tension (P_0). Experimental maximum shortening velocity (V_{EXPmax}), at the preload (pL) required to obtain L_{max}, was measured. The maximum unloaded shortening velocity (V_{max}) was computed by means of Hill's equations (Coirault et al., 1995): $(P + a)(V + b) = (P_0 + a)b$, where a and b represent the asymptotes of the hyperbola and P_0 is the peak isometric tension for $V = 0$. The V_{max} was obtained from the ordinate intercept and calculated as P_0b/a. The shortening velocity was normalized to L_{max}.

The curvature of the force–velocity relationship (G) was calculated as P_0/a. In striated muscle the G value reflects the myothermal economy (i.e., the higher the G the more economical the contraction). The maximum mechanical efficiency (Eff_{max}) has been defined as the maximum ratio of mechanical work performed during contraction to the total free energy change of the mechanical process involved in contraction. As previously described (Coirault et al., 1995), the calculation of Eff_{max} was derived from Hill's equation according to the following: $Eff_{max} = [G/(G + 2)]^2$.

2.5 | Crossbridge characteristics

Huxley's mathematical model of muscle mechanics provides an informative system for estimating the number ($\psi \times 10^9$), unitary force (Π_0) and kinetics of myosin crossbridges (CB) in living muscles. Huxley's formalism not only accounts for many macroscopic hallmarks of muscle (force velocity and heat production) but also relates these characteristics to their structural and biochemical properties. According to the mathematical model, force and shortening in muscle are generated by cycling interaction of the myosin head with specific sites on the thin filament, with ATP hydrolysis providing the energy (Lecarpentier et al., 1998). By using mechanical parameters (velocity, length, force) of the entire muscle at various load levels, Huxley's theory infers the kinetics and number of CBs (Blanc et al., 2003). Thus, the use of Huxley's formalism seems to be an adequate way of investigating whether changes in mechanical motor performance of diabetic PM could be attributed to differences in CB interactions. According to the most widely accepted theory of contraction (Huxley & Simmons, 1971a), muscle force depends on the unitary CB force and the total number of CBs. Considering the values of Huxley's equation parameters h (crossbridge step size equal to 11 nm), e (free energy required to split one ATP molecule equal to 5.1×10^{-20} J), l (the distance between two actin sites equal to 36 nm) and w (the maximum mechanical work of a unitary crossbridge equal to 3.8×10^{-20} J), it is possible to compute the peak values of the rate constants for CB detachment g_1 and g_2 (s^{-1}) and the maximum value of the rate constant for CB attachment f_1 (s^{-1}):

$$g_2 = \frac{2V_{max}}{h}$$

$$g_1 = \frac{2wb}{ehG}$$

$$f_1 = \frac{-g_1 + \sqrt{g_1^2 + 4g_1g_2}}{2}$$

This approach allows calculation of the unitary force per CB (Π_0, pN) and the number of CB ($\Psi \times 10^9$) per mm^2 at P_0:

$$\Pi_0 = \frac{w}{l} \times \frac{f_1}{f_1 + g_1}$$

$$\psi = ab/e\frac{h}{2l} \times \frac{f_1 g_1}{f_1 + g_1}$$

2.6 | Ultrastructural study

Anterior left ventricular PM was quickly fixed with 1% paraformaldehyde and 1.25% glutaraldehyde in 0.15 M cacodylate buffer for 2 h at room temperature for transmission electron microscopy (TEM). During fixation, to maintain left ventricular PM at L_{max}, specimens were hung in the fixative with a weight on the bottom end, consistent with preload at L_{max} obtained during the length–tension relationship. Samples were then treated for conventional TEM preparation (Isola et al., 2013; Loy et al., 2014; Riva et al., 2011). Briefly, fixed tissues were post-fixed in 2% osmium tetroxide and left in 0.5% uranyl acetate overnight. They were then dehydrated, embedded in Epoxy resin and then cut in an ultramicrotome. Semithin sections (1 μm) for light microscopy (LM) were stained with toluidine blue or ultrathin slices (80–90 nm) for TEM were contrasted with uranyl acetate and bismuth subnitrate. TEM samples were observed in a JEOL 100S TEM, while LM images were acquired by a Leica (Wetzlar, Germany) microscope equipped by a CCD camera.

Image analysis was performed on both TEM and LM digital images using the ImagePro plus software (NIH, Bethesda, MD, USA).

In LM analysis five hearts of control animals and six hearts of diabetics were examined. For each experimental category, a total of 300 measurements were collected on a total of 25–35 pictures.

The number of sarcomeres counted was normalized to that within one unitary length of 10 μm. Longitudinal sectioning was deemed to be adequate when the z lines of cardiomyocyte myofibrils were evident.

TEM morphometry was performed on five control and six diabetic hearts. A total of 27 or 34 micrographs were acquired for control and diabetic samples, respectively, and per each image 3–18 measurements were performed, which were averaged as one value per photo. Sarcomere length was measured only when fibres were sectioned on a parallel plane to the myofibril axis, that is, when it was possible to draw a line between two z-lines, which superimposed myofilaments, resulting in a 90° angle on both sides. Moreover, manifestly contracted sarcomeres were excluded from measurement. A-bands were measured on the same images from one border between the A- and I-band to the next one. Data are shown as means ± SD.

2.7 | Immunoblotting

Left ventricle tissues from five diabetics and six controls rats were homogenized in 10 mM Tris pH 7.4, 5 mM EDTA, 1% Triton X-100, 1% Nonidet P-40, to which 1:100 protein inhibitor cocktail was added (Sigma-Aldrich, St Louis, MO, USA), centrifuged at 500 g for 10 min, and then the supernatant was collected. Protein content was checked by the Lowry method. For denaturation, 50 μg of proteins was heated for 15 min at 72°C (50:50 v/v) in 4% SDS, 20% glycerol, 160 mM dithioerythrol, 125 mM Tris-Cl (pH 6.8), bromophenol blue 0.004%. Sample proteins were then separated by electrophoresis on 4–15% Mini-PROTEAN TGX precast polyacrylamide gels (Bio-Rad Laboratories, Hercules, CA, USA), and then transferred on polyvinylidene difluoride membranes, which were blocked with 5% milk in Tris-buffered saline with 0.1% Tween 20 (TBS-T) overnight. The following antibodies were then used: rabbit anti-collagen type I (Millipore, Billerica, MA, USA, dilution 1:2000); rabbit anti-collagen type III (Biorbyt, Cambridge, UK, dilution 1:1000); mouse anti-β-myosin heavy chain (MHC) (Sigma-Aldrich M8421, dilution 1:4000). Anti-collagen I and III antibodies had an overnight incubation at 4°C, whereas for anti-β-MHC incubation time was 3.5 h at room temperature. Secondary antibodies (goat anti-rabbit peroxidase conjugate 1:1500, for anti-collagen I and III, or rabbit anti-mouse peroxidase conjugate 1:1000, for anti-β-MHC and anti-β-tubulin, both from Sigma-Aldrich) were incubated for 1.5 h at room temperature. Detection of protein signals was achieved by using the ECL Prime chemiluminescence kit (GE Healthcare) and images acquisition using a Fujifilm Luminescent Image Analyzer LAS4000 System (Fujifilm, Tokyo, Japan). Immunoreactive bands were analysed for densitometry with Image Studio Lite Software (LI-COR, Lincoln, NE, USA). Protein quantification was expressed as the relative intensity of protein signals ratioed with the expression of the housekeeping gene for β-tubulin (Sigma-Aldrich, dilution 1:2000).

2.8 | Statistics

On physiological, morphometric and immunoblotting data, statistical evaluation was performed by applying an unpaired two-tailed Student's t-test on selected pairs with GraphPad Instat software (GraphPad Software, Inc., La Jolla, CA, USA), with previous assessment of normal distribution. A value of $P < 0.05$ was considered statistically significant.

3 | RESULTS

3.1 | Animal model

One week after streptozotocin injection, female rats had developed DM as displayed by a statistically significant increase in plasma glucose concentration (382 ± 20 mg dl^{-1} in the diabetics vs. 97.90 ± 0.1 mg dl^{-1} in the control rats; $P < 0.001$). The diabetic condition was maintained until the end of the experimental period, as revealed by the presence of increased level of blood ketone bodies, cornea opacities and a failure to gain weight, despite an increased intake of both water and food. Table 1 shows comparisons of the general features between control and diabetic rats, following about 20 weeks of observation. Diabetic rats were significantly lighter and showed increased food and water

TABLE 1 General features of control and diabetic rats

	Controls	Diabetics
Blood glucose (mg dl^{-1})	90.7 ± 3.2	487.0 ± 13.1**
Blood ketones (mg dl^{-1})	0.67 ± 0.1	1.13 ± 0.3**
Body weight (g)	262.5 ± 16.1	211.5 ± 25.9**
Food intake (g die^{-1})	15.4 ± 2.2	31.0 ± 1.6**
Water consumption (ml die^{-1})	31.2 ± 4.1	119.2 ± 11.4**

Values are expressed as means ± SD, $n = 20–29$ per group, $^{**}P < 0.001$, unpaired Student t-test.

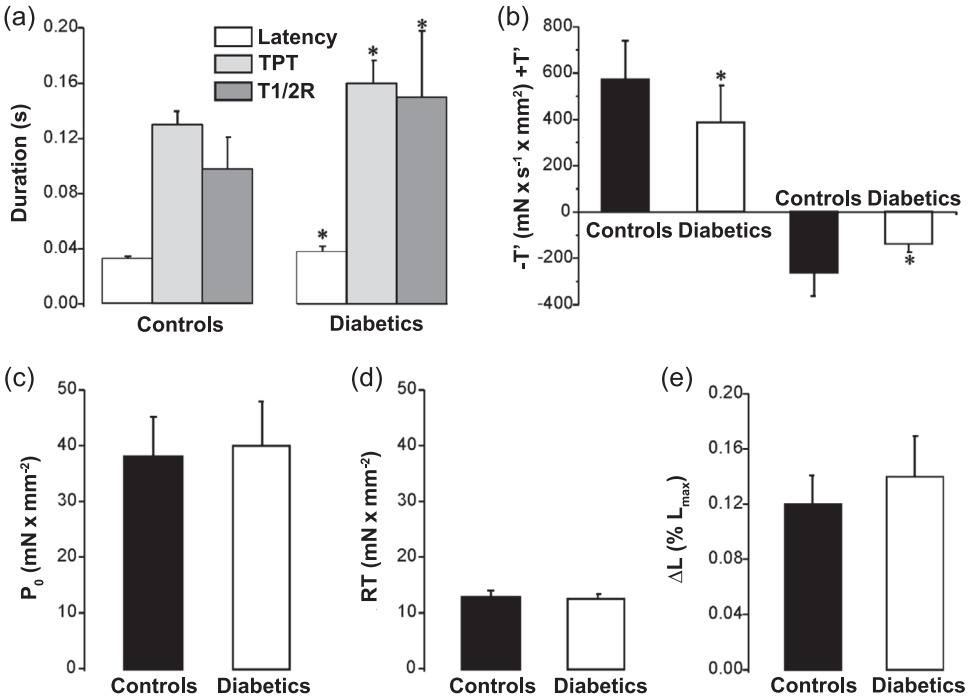

FIGURE 1 Isometric and isotonic contraction parameters in control and diabetic rats. (a) The most striking differences of isometric timing parameters: latency (time of latency), TPT (time to peak tension) and T½R (half-time of relaxation) were significantly prolonged in diabetic papillary muscle. (b) +T′ (peak rate of tension rise) and −T′ (peak rate of tension fall) were significantly slower in diabetic animals. (c, d) Isometric parameters: P_0 (peak isometric tension) and RT (resting tension). (e) Isotonic parameter: ΔL: maximum extent of shortening. $n = 13–16$ hearts per group and 1 papillary muscle per heart. Values are expressed as means ± S.D; $^{*}P < 0.05$

intake compared to control rats ($P < 0.001$) in agreement with previous reports on diabetic animal models (Kita et al., 1991; Brown et al., 2001; Howarth et al., 2000). All diabetic rats survived throughout the experimental period.

3.2 | Isometric and isotonic studies

Figure 1 shows the most striking differences of isometric timing parameters at L_{max} and 0.06 Hz of control and diabetic rats. As shown in Figure 1a, latency, TPT and T½R were all significantly prolonged in diabetic PM compared to control ($P < 0.05$): latency was 0.038 ± 0.004 versus 0.033 ± 0.002 s, TPT was 0.159 ± 0.02 versus 0.136 ± 0.01 s and T½R was 0.146 ± 0.048 versus 0.098 ± 0.024 s in diabetic and control rats, respectively. +T′ and −T′ were significantly slower in diabetic compared with control animals (Figure 1b, $P < 0.05$). All these indexes of contraction and relaxation were altered in diabetics compared to control, suggesting a hidden papillary contractility impairment. By contrast, the other mechanical experimental parameters, P_0, RT and ΔL, of left ventricular PMs did not reveal any difference between the groups: P_0 was 39.91 ± 8.14 versus 38.08 ± 7.07 mN mm^{-2} and RT was 12.72 ± 0.98 versus 12.92 ± 1.17 mN mm^{-2} in diabetic and control rats, respectively (Figure 1c, d). ΔL was 0.14 ± 0.03 versus 0.12 ± 0.02% L_{max} (Figure 1e) in diabetic and control rats, respectively.

3.2.1 | Force–frequency relationship

Figure 2 shows the influence of stimulation frequency on isometric mechanical and timing parameters in the control and diabetic rat

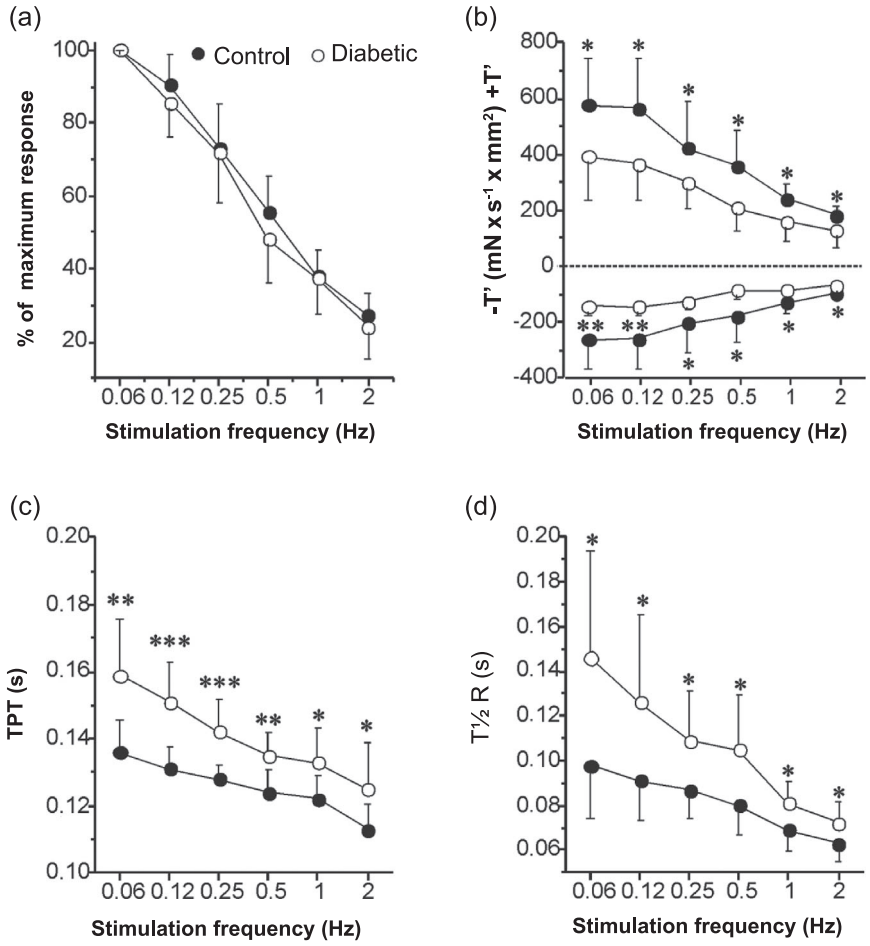

FIGURE 2 Influence of the stimulation frequency on contraction and the timing parameters in control and diabetic groups. Filled symbols show data from control rats ($n = 13–16$ hearts per group and 1 papillary muscle per heart); open symbols show data from matched diabetics ($n = 13–16$ hearts per group and 1 papillary muscle per heart). (a) Peak isometric tension, expressed as percentage of maximum response, was not different between groups. (b–d) Timing parameters: +T′ (peak rate of tension rise) and −T′ (peak rate of tension fall), TPT (time to peak tension) and T½R (half-time of relaxation). Values are expressed as means ± SD; $^{*}P < 0.05$, $^{**}P < 0.01$, $^{***}P < 0.001$

PM. In general, in both groups, all measured parameters showed a negative FFR characterized by their decrease in response to an increase in stimulation frequency (0.06, 0.12, 0.25, 0.5, 1 and 2 Hz). There were no differences in peak isometric tension, P_0, expressed as a percentage of maximum response, between control and diabetic rats at all frequencies tested (Figure 2a). As observed in Figure 2b, +T′ and −T′ were significantly slower in the diabetic group when compared with the control group at all frequencies tested (for +T′ $P < 0.05$ at all frequencies; for −T′ $P < 0.01$ at 0.06 and 0.12 Hz and $P < 0.05$ at the other frequencies), and TPT and T½R were significantly prolonged in the diabetic group when compared to control group (Figure 2c–d) (for TPT $P < 0.01$ at 0.06 and 0.5 Hz, $P < .0.001$ at 0.12 and 0.25 Hz, and $P < 0.05$ at 1 and 2 Hz; for T½R $P < 0.05$ at all frequencies).

3.2.2 | Force–velocity relationship

Mechanical and energetic parameters of PM are depicted in Figure 3. As compared to control, diabetic rats exhibited a decreased V_{EXPmax} (0.86 ± 0.11 vs. 0.97 ± 0.13 L_{max} s^{-1}, $p < 0.05$; Figure 3a). The average force–velocity curves obtained in the LV papillary muscle in control and diabetic groups partially overlap with the exception of V_{max}. Indeed, the V_{max} was slower in diabetic rats when compared to controls (0.91 ± 0.15 vs. 1.04 ± 0.16 L_{max} s^{-1} respectively, $P < 0.05$; Figure 3b). Both G (curvature of the force–velocity hyperbola) and the peak mechanical efficiency were significantly smaller in the diabetic group than in the control group (G curvature: 0.42 ± 0.10 vs. 0.55 ± 0.13, respectively, $P < 0.01$, Figure 3c; Eff_{max}: 0.031 ± 0.013 vs. 0.05 ± 0.025, respectively, $P < 0.05$; Figure 3d).

3.3 | Myosin number of crossbridges, force and kinetic

CB number at P_0, Ψ (10^{11} mm^{-2}), unitary force per CB, Π_0 (pN) and myosin CB kinetics are illustrated in Figure 4. At the CB level, compared to control rats, PM from diabetic rats exhibited higher Ψ (~ 35%, $P < 0.05$; Figure 4a). However, Π_0 was significantly lower in the diabetic group if compared to control one (~ 20%, $P < 0.05$; Figure 4b). The cycle duration, Tc, (Figure 4c) was significantly higher in the diabetic group than in the control one (0.011 ± 0.004 vs. 0.007 ± 0.001 s, respectively, $P < 0.05$). Finally, the diabetic group exhibited a decreased maximum turnover rate of myosin ATPase, K_{cat} (Figure 4d) per site in isometric conditions as compared to the control group ($P < 0.05$).

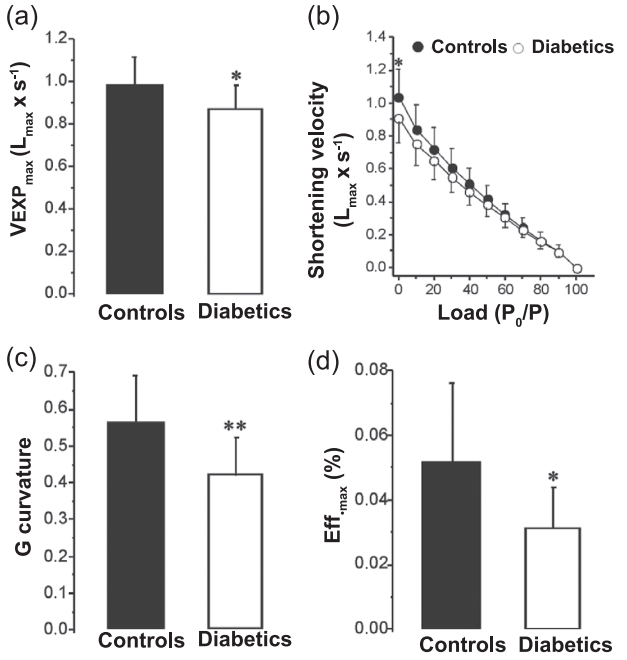

FIGURE 3 Kinetics and energetic parameters in control and diabetic rats. (a, b) Significantly decreased V_{EXPmax} (experimental maximum shortening velocity at preload) in diabetics. (b) Average *F–V* curves. (c, d) *G* (curvature of the force–velocity hyperbola) and Effmax (peak mechanical efficiency). ($n = 13–16$ hearts per group and 1 papillary muscle per heart.) Values are expressed as means ± SD; $^*P < 0.05$, $^{**}P < 0.01$

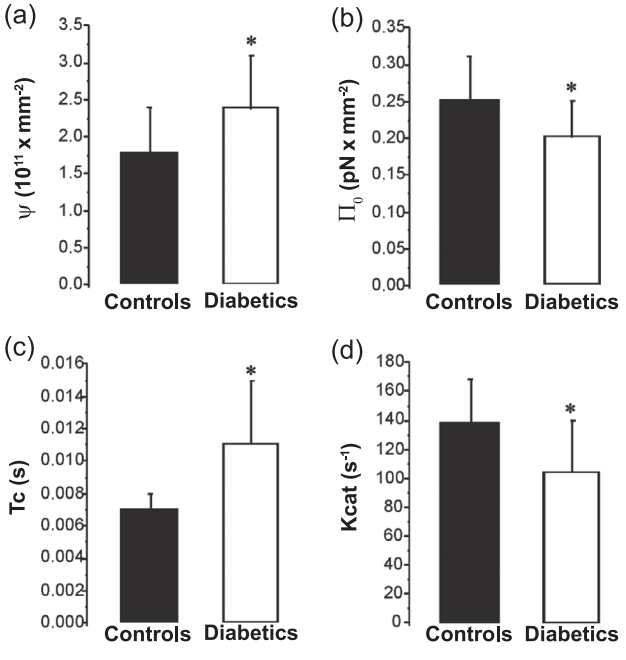

FIGURE 4 Myosin crossbridge number, force and kinetics in control and diabetic rats. (a, b) Diabetes-induced acto-myosin interaction changes. At peak isometric tension, Ψ (total number of crossbridges) was significantly higher and Π_0 (unitary crossbridge force) was significantly smaller in diabetics. (c, d) The crossbridges cycle duration (Tc) was significantly prolonged in diabetics as supported by a slower maximum turnover rate of myosin ATPase per site (K_{cat}). ($n = 13–16$ hearts per group and 1 papillary muscle per heart.) Values are expressed as means ± SD, $^*P < 0.05$

3.4 | Histological and ultrastructural studies

LM images of control PM showed regularly shaped cardiomyocytes, normal intercalated disk appearance, capillary distribution, connective cell occurrence and extracellular matrix arrangement (Figure 5a). Observation of diabetic samples (Figure 5b) revealed no morphological difference between control and diabetic rats. Morphometric analysis on LM images showed that, compared to control, diabetes lowered the number of sarcomeres per 10 μm length (4.55 ± 0.02 vs. 4.69 ± 0.03, $P < 0.05$).

TEM images of papillary muscles exhibited the typical cardiomyocyte ultrastructure with variable sized myofibrils intercalated to two different types of mitochondria: subsarcolemmal mitochondria, which were juxtaposed to sarcolemma, and interfibrillar mitochondria, which were intermingled with myofibrils (Figure 5c, d). As in the case of LM images, ultrastructural analysis did not highlight any apparent difference between control (Figure 5c) and diabetic (Figure 5d) rats. Myofibrils were in register, and on them the appearance of sarcomeres was regular with evident Z lines, A- and I-bands. Overall, cardiomyocyte inner morphology was not different in control and diabetic rats. After morphometric analysis of TEM micrographs, it was evident that diabetes induced some differences: diabetic myofibrils had longer sarcomeres (2.56 ± 0.26 μm in the diabetic group vs. 2.33 ± 0.35 μm in the control $P < 0.01$; Figure 6a) and longer A-bands compared to control ones (1.92 ± 0.15 μm in the diabetic group and 1.83 ± 0.18 μm in the control group, $P < 0.05$; Figure 6b).

3.5 | Immunoblotting

To confirm that our diabetic model did not alter the expression of connective tissue proteins, we searched for cardiac collagen I and III content by immunoblotting (Figure 7a, b). The results, confirming LM and TEM observation, showed that neither collagen I nor collagen III content increased in rat hearts following a diabetic condition maintained for almost 5 months.

In diabetic and control rats we also investigated the expression of the slow form of myosin, β-MHC (Figure 7c). Immunoblotting data revealed a statistically significant two-fold increase of β-MHC content in diabetic as compared to control rats (4.45 ± 2.06 vs. 2.29 ± 1.13 a.u.; $P < 0.05$).

4 | DISCUSSION

The present study delineated the effect of DM on left ventricular PM contractility in STZ-treated rats. In terms of intrinsic muscle function, left ventricular PMs from diabetic rat hearts would seem to manifest

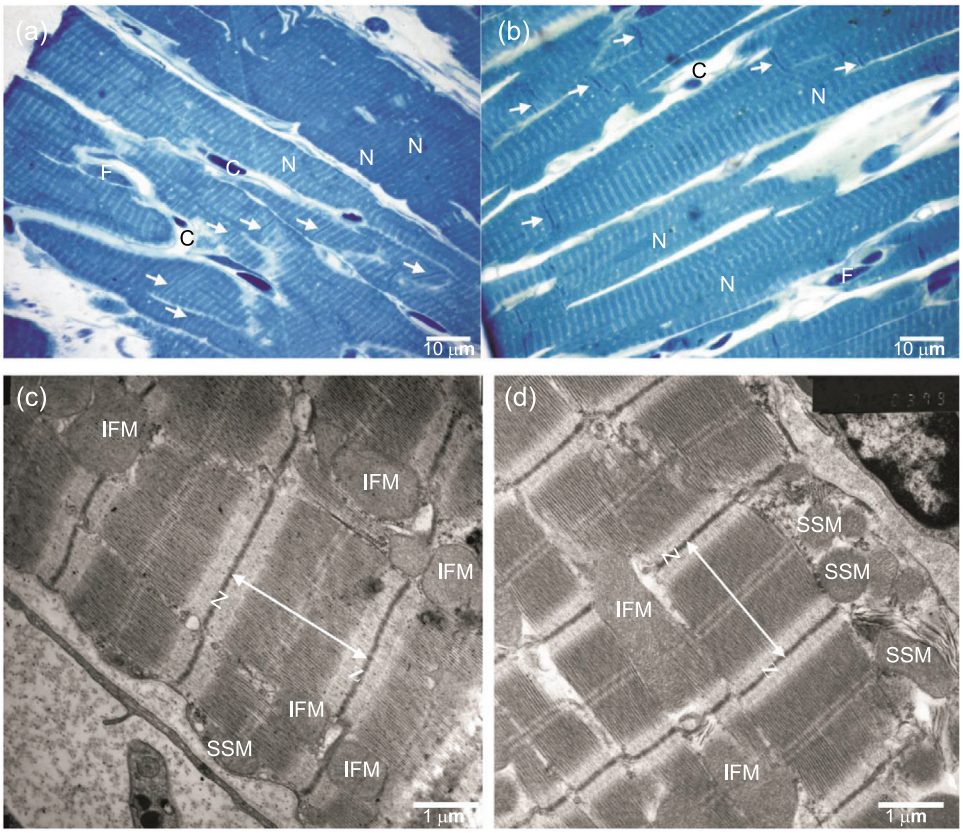

FIGURE 5 Histological and ultrastructural features. Morphological features of normal and diabetic myocardium by light microscopy (LM) (a, b) and transmission electron microscopy (TEM) (c, d). Control (a) and diabetic samples (b) display no morphological differences by LM. Cardiac myocytes showed normal histological features with central nuclei (N), abundant intercalated discs (arrows), and a normal amount of interposed connective tissue with fibroblasts (F) and capillaries (C). (c, d) TEM micrographs of papillary muscles (c, control; d, diabetic) showing regular myofibrils that are bordered by a plethora of mitochondria (both subsarcolemmal, SSM, and interfibrillar, IFM). Ultrastructural features were not different in control and diabetic animals. Myofibril observation reveals normally oriented, not contracted sarcomeres. Sarcomere length was measured from one z-line (Z) to the next one, and the A-band, which includes myosin thick filaments, is shown by the double arrowed line in both micrographs

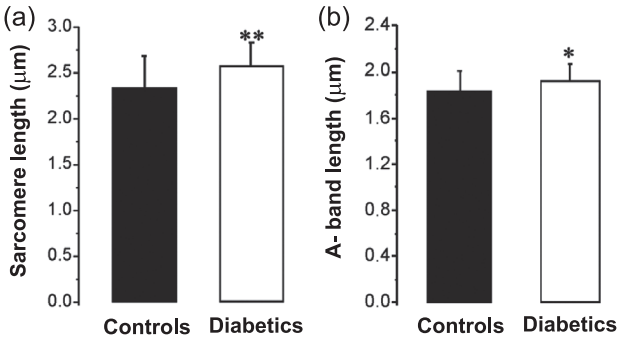

FIGURE 6 Morphometry on TEM images. (a) Measurements of sarcomere length in control and diabetic rats. A prolonged diabetic condition increased sarcomere length versus controls. (b) Measurements of A-band length within the sarcomeres of papillary muscles of control and diabetic rats. Diabetic animals possessed longer A-bands than controls. Values are expressed as means ± SD, $n = 27–34$ averaged values, 5–6 hearts per group; $^{*}P < 0.05$, $^{**}P < 0.01$ unpaired *t*-test

slower contraction and relaxation, but no change in maximal active tension. Indeed, in our experimental results, the isolated diabetic PM showed: (1) a prolonged time of latency and time to peak tension plus a delayed onset of relaxation as measured by the half-time of relaxation; and (2) a significant slowing of the timing parameters +T′ and −T′. Similar results were also obtained for FFR, where the same findings in contraction and relaxation indexes were maintained even at the highest stimulation frequency applied (2 Hz). Moreover, an important change in the energetics of the diabetic PMs was the depression of V_{EXPmax} and V_{max}. These observations confirmed that diabetes prolonged the time courses of both contraction and relaxation processes, and this might lead to the diastolic dysfunction observed in diabetes (Basu et al., 2009) and eventually result in heart failure with preserved ejection fraction (Lindman, 2017).

To our knowledge, impaired contractility secondary to diabetic cardiomyopathy has been ascribed to different calcium sensitivity, altered expression of β-MHC and different phosphorylation of regulatory proteins of myosin head displacement.

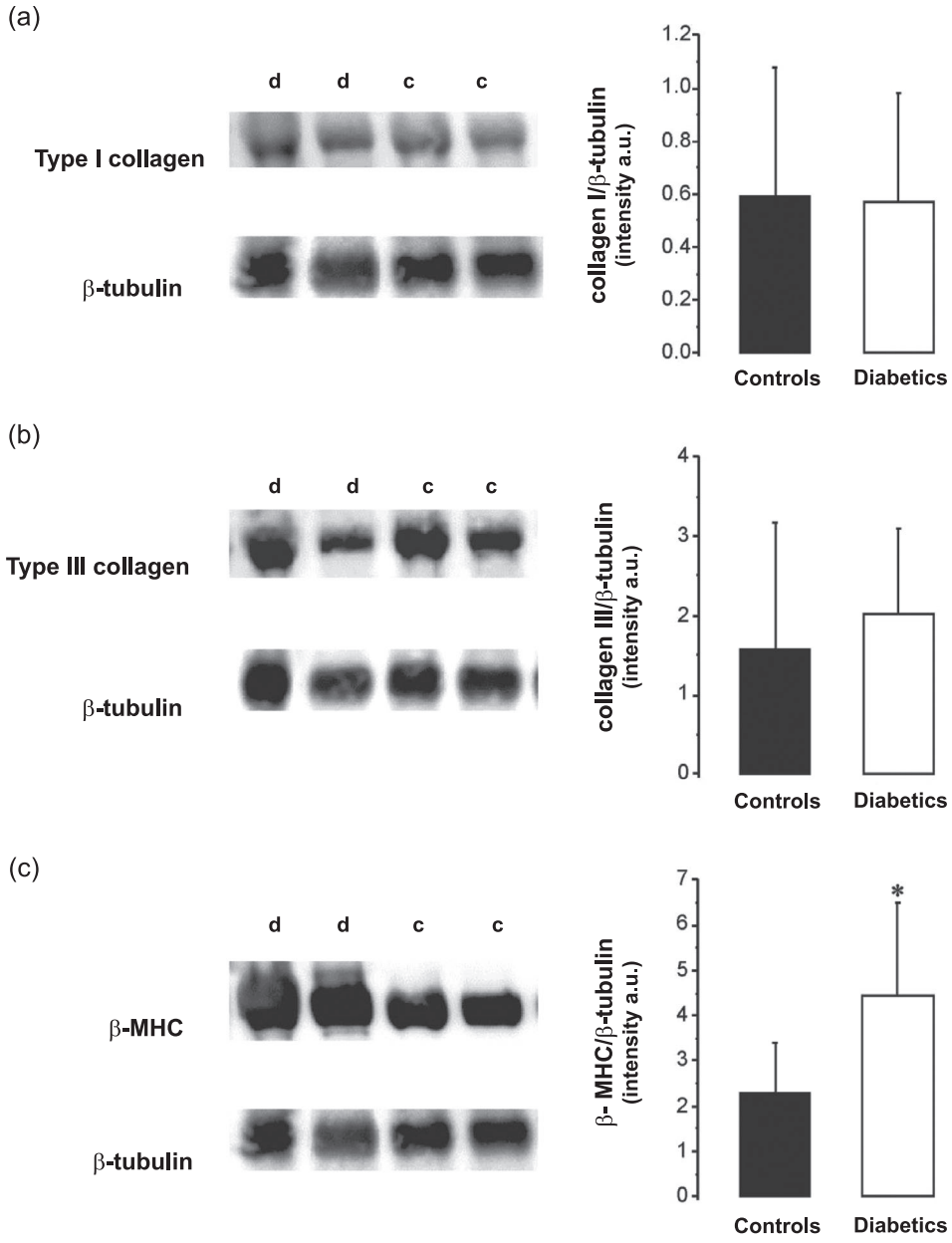

FIGURE 7 Immunoblotting results on left ventricle tissues. (a) Immunoblotting for type I collagen did not reveal a change in collagen content between control and diabetic rats. (b) Type III collagen had a slight tendency to increase after diabetes, but that was not statistically significant. (c) Diabetes markedly increased β-MHC protein expression as compared to controls ($P < 0.05$ unpaired t-test). $n = 5–6$ hearts per group

The contractile defects correlated to contraction and relaxation processes observed in our diabetic PMs have been usually associated to abnormal intracellular calcium homeostasis leading to an excitation–contraction uncoupling. Slowed rates of contraction and relaxation in diabetics have been attributed to an impairment of Ca^{2+}-regulating proteins, such as SERCA, the ryanodine receptor and the sarcolemmal Na^{+}/Ca^{2+} exchanger (Chattou et al., 1999). More recently, it has been demonstrated that these defects did not affect intracellular calcium concentration, because in diabetic hearts, an increase in left ventricular action potential duration would compensate the decreased sarcoplasmic reticulum calcium uptake, ensuring the maintenance of sarcoplasmic calcium content (Zhang et al., 2008).

Despite these abnormalities, biomechanical parameters of diabetic PM, such as P_0, RT and ΔL, were maintained, as already observed in other studies (Fein et al., 1980; Han et al., 2014; Kita et al., 1991).

Since P_0 also depends on the degree of myofilaments' overlapping and consequently on the number of active of crossbridges (Blanc et al., 2003; Huxley & Simmons, 1971b), we have verified whether the maintenance of biomechanical behaviour in the diabetic PMs, representing probably a mechanism adaptive to the diabetic state,

could be also related to a modification of sarcomeres, in terms of interactions of their associated proteins.

In keeping with that, our morphological and morphometric studies assessed that in diabetic myofibrils fewer and longer sarcomeres and, within sarcomeres, longer A-bands were detected compared to controls. Furthermore, using theoretical equations of Huxley's mathematical model, we have estimated a 35% increase in the total number of active crossbridges per mm^2 but a 20% reduction in the unitary force per crossbridge in diabetic PMs as compared to control ones.

Our results are at variance with what was reported in the paper of Joseph and colleagues (2005) as far as crossbridge number, their unitary force and P_0 in diabetic PMs are concerned. They found a lower crossbridge number and no change in crossbridge unitary force in diabetics as compared to controls. The work by Joseph and colleagues was analogous to ours in the physiological protocol and in the application of the Huxley mathematical model, but differed in that they used male rats and investigated a shorter period of diabetes (13 weeks against about 20 weeks).

In our findings, the similar value of P_0 and ΔL in control and diabetic left ventricular PMs is of prime importance because it allows us to infer that blood ejection from the ventricular chamber would be preserved during systole. We should point out that our interpretation is mode-dependent because it is constrained by the limits of isolated organ conditions. On the other hand, in agreement with our consideration, Siri et al. observed a correlation between isolated papillary muscle function and ventricular performance *in situ* in the same animal model of renal hypertensive diabetic rat. Indeed, they propose that the same intrinsic myocardial alterations, such as prolongation of left ventricular PM contraction–relaxation, would promote preservation of a relatively normal cardiac output as opposed to diminishing contractile speed, in the intact diabetic heart (Siri et al., 1997).

The relationship between the maximum velocity of shortening and myosin isoenzyme pattern in rat heart has been well established (Falcão-Pires & Leite-Moreira, 2012; Malhotra & Sanghi, 1997). DM is associated with shifts in cardiomyocyte contractile machinery, from α (fast contracting) to β (slow) myosin heavy chain isoform consistent with a decrease in myofibrillar ATPase activity (Dhalla et al., 1998; Malhotra & Sanghi, 1997). Accordingly, we found that diabetes triggered a robust increase of β-MHC content, which should sensibly modify contractility dynamics (Krenz & Robbins, 2004). Indeed, our findings showed that the turnover rate of myosin ATPase activity per crossbridge (K_{cat}) was lower in diabetics than in controls and considering that changes in K_{cat} have been also correlated with the G curvature and the maximum mechanical efficiency (Alpert & Mulieri, 1982; Lecarpentier et al., 1987; Woledge et al., 1985), we confirmed that the calculated decrease in G and Eff_{max} of diabetic rats could be related to the development of alterations in contractile efficiency.

Morphometric measurements on TEM images revealed that sarcomeres increased their length by about 10% in diabetic compared with control animals. Analogous measurements on the A-band showed an increase of about 5%. Thus, we may infer that also I-bands increased their length by 5%, matching the increase of A-bands and, probably, making functional acto-myosin interactions. Thus, the reported increase in β-MHC content is consistent with an elongation of A-bands. Moreover, by applying Huxley's formalism, we detected a 35% increase of the active crossbridges, which is higher than the recorded percentage in sarcomere elongation. Hence, some other mechanism might account for this increase. We can put forward the hypothesis that the recruitment of new crossbridges arose from a shift from the super-relaxed myosin (SRX) state, an inactive form of myosin where myosin heads are bound to the thick filament and incapable of making crossbridges with actin filaments, to the disordered myosin (DRX) state (in which myosin binds to the thin filament with a lower ATP turnover rate) first and/or then into active myosin (Schmid & Toepfer, 2021). Alternatively, an increase in crossbridge number might come from phosphorylation of cardiac myosin-binding protein C (cMyBP-C) a protein that, once phosphorylated, brings myosin closer to the thin filament, optimizing acto-myosin interaction and, ultimately, increasing crossbridge number (Brunello et al., 2020; Schmid & Toepfer, 2021). Usually, cMyBP-C acts like a break, and only after phosphorylation enhances crossbridge kinetics (Van der Velden & Stienen, 2019). Since our kinetics are reduced, we might hypothesize that cMyBP-C was not phosphorylated and was not involved in diabetes contractility. A further protein involved in the activation of SRX is the regulatory light chain (RLC) site in on the myosin molecule. It has been proved that in heart muscle, phosphorylation of RLC brings myosin heads into an ordered state (i.e. ready to bind to actin filament) (Kampourakis & Irving, 2015). Myosin light chain kinase is the enzyme which phosphorylates RLC, and it was reported that diabetes decreased it by about 30% (Liu et al., 1997). However, that work is related to streptozotocin-treated male rats, studied only 8 weeks after the development of diabetes. Therefore, we cannot exclude that in our female rats after about 20 weeks of diabetes this mechanism could have had a pivotal role.

Shifts from the SRX to DRX state of myosin have been related to hypercontractility in hypertrophic cardiomyopathy but are also exploited in new drugs, such as omecamtiv mecarbil, used as cardiac activators (Anderson et al., 2018). This double character of SRX involvement will be useful to understand the development of cardiomyopathies in future studies.

The lower unitary force developed by a single myosin head in diabetic as compared to control rats observed in the present study was discordant with previous findings demonstrating that α and β cardiac myosin isoforms exhibited similar force generating capacity (Malmqvist et al., 2004; Palmiter et al., 1999; Sugiura et al., 1996). A decrease in crossbridge unitary force has also been related to increased cycling rate of crossbridges (Fenwick et al., 2019). As we found that diabetes decreased K_{cat}, we might infer that this mechanism was not responsible for the calculated decrease of unitary force in diabetic animals. Hence, our data do not allow us to explain why diabetic PMs developed lower elementary force per myosin head than control ones.

Despite the development of diabetic cardiomyopathy often being correlated to an increase of interstitial fibrosis in myocardial tissue, in our model of DM we did not detect any sign of enhanced

deposition of interstitial matrix. Indeed, both our immunoblotting and histological findings highlighted no evidence of collagen I and III overexpression and their accumulation between diabetic cardiomyocytes. Some authors have shown no change of collagen deposition in the cardiovascular system of type-I diabetes animal models (Litwin et al., 1990), and sometimes this lack of fibrosis was concomitant to diastolic dysfunction (Basu et al., 2009). Moreover, there is the possibility that a tendency for diabetic collagen oversecretion could be compensated by an increase of its specific proteases, such as matrix metalloprotease 2, which has been reported to be overexpressed in diabetes (Bupha-Intr et al., 2011). This result agrees with our isometric experimentally measured parameters that revealed also an unaffected resting tension in isolated PM, consistent with other works (Fein et al., 1980; Litwin et al., 1990). Although the absence of augmented interstitial collagen deposition alone may explain the unaltered resting tension, we cannot exclude that sarcomeric titin might have shifted towards the more compliant isoform, an event that has been also correlated with an unchanged passive tension in diabetic hearts (Krüger et al., 2010; Zile et al., 2015).

Lastly, in our interpretation, diabetes-induced modifications, such as the augmented β-MHC content, increased sarcomere length and cross-bridge number enhancement, are features that preserve myocardial stroke and could concur to maintain the ejection fraction. Indeed, despite crossbridges of diabetic PMs developing a lower unitary force compared to control ones, the greater sarcomere length and a slower kinetics preserved papillary contractile function.

Energetic analysis derived from the force–velocity relation provides a theoretical approach leading to a calculation of mechanical efficiency. Based on theoretical analyses by Hill (1964), the force–velocity relationship has been extensively used to evaluate mechanics and energetics of isolated muscle (Alpert & Mulieri, 1982; Lecarpentier et al., 1987; Woledge et al., 1985). Our theoretical approach thus closely fits with experimental data derived from biochemical (ATPase activity), thermodynamic techniques (Woledge et al., 1985) and with muscle theory (Chattou et al., 1999).

In our study, the CB number and elementary force per CB were calculated from mechanical data using A. F. Huxley's formalism (Huxley & Simmons, 1971b). The principles of Huxley's theory were based on experiments performed on isolated frog sartorius muscles under tetanus conditions, and not on rat isolated papillary muscles during twitch contraction. Moreover, our experimental data are in perfect agreement with Huxley's equations, and therefore it is reasonable that these equations can be applied in our study and that the obtained data might be considered accurate and reliable.

In addition, female rats were chosen in our experimental diabetic model as primary experimentation propaedeutic to a more complete study, in which a comparison of the diabetic effect on the cardiovascular system between male and female rats will be considered. Although the incidence of heart diseases in diabetic men and women is 2 and 5 times higher, respectively, when compared with their age-matched healthy counterparts (Sowers, 1998), a growing body of evidence has suggested that there is a sex bias in the onset of diabetic cardiomyopathy. Indeed, premenopausal women frequently have a lower risk of cardiovascular diseases than age-matched men and postmenopausal women. Also, heart failure with preserved cardiac function is more frequent in female than male diabetic patients (Regitz-Zagrosek & Kararigas, 2017).

One limit of this study is that it cannot be directly translated to humans, because of differences in the distribution of the contractile proteins such as α and β-MHC in humans and rats. In humans 90% of myosin is in the β-MHC form and only 10% is represented by α-MHC (Locher et al., 2009). On the contrary, in rat myocardium it is reported that the composition is 65% α-MHC and 35% β-MHC. Nonetheless, we recorded a relevant increase in β-MHC that can mimic a small shift in the human β-MHC content, which is reported to occur in type I diabetes and to dramatically change kinetics of contraction. Moreover, a rat model of streptozotocin-induced diabetic cardiomyopathy is still widely employed for the evaluation of the mechanisms that induce this pathology.

In conclusion, for the first time, we showed that type-I diabetes altered sarcomeric ultrastructure, as seen by TEM, consistent with physiological parameters. The diabetic condition induced slower timing parameters, which is consistent with diastolic dysfunction. In tandem with this, at the sarcomeric level, augmented β-MHC content and increased sarcomere length and crossbridge number preserve myocardial stroke and could concur to maintain the ejection fraction.

ACKNOWLEDGEMENTS

We thank A. Capra for technical assistance. This study was supported by the Sardinian Region Government (RAS), L.R. 7/2007, Grant CRP 366 60052 (R.V. and R.I.).

COMPETING INTERESTS

The authors declare no conflict of interest.

AUTHOR CONTRIBUTIONS

The original idea for the study came from R.V. and R.I. R.V. and R.I. initiated the study, planned the experimental approach and designed the experiments. R.V. and F.B. performed physiological experiments. R.I. and A.C. performed morphological experiments. A.C. performed image analysis and statistics. M.I. and F.L. provided technical assistance. R.V., R.I. and F.B. wrote the paper. All authors have read and approved the final version of this manuscript and agree to be accountable for all aspects of the work in ensuring that questions related to the accuracy or integrity of any part of the work are appropriately investigated and resolved. All persons designated as authors qualify for authorship, and all those who qualify for authorship are listed.

DATA AVAILABILITY STATEMENT

All data generated or analysed during this study are included in this published article and are available from the corresponding author on reasonable request.

ORCID

Romina Vargiu https://orcid.org/0000-0001-6994-8105

REFERENCES

Alpert, N. R., & Mulieri, L. A. (1982). Myocardial adaptation to stress from the viewpoint of evolution and development. *Society of General Physiologists Series*, *37*, 173–188.

Anderson, R. L., Trivedi, D. V., Sarkar, S. S., Henze, M., Ma, W., Gong, H., & Spudich, J. A. (2018). Deciphering the super relaxed state of human β-cardiac myosin and the mode of action of mavacamten from myosin molecules to muscle fibers. *Proceedings of the National Academy of Sciences, USA*, *115*(35), E8143–E8152. https://doi.org/10.1073/pnas.1809540115

Ares-Carrasco, S., Picatoste, B., Benito-Martín, A., Zubiri, I., Sanz, A. B., Sánchez-Niño, M. D., & Lorenzo, O. (2009). Myocardial fibrosis and apoptosis, but not inflammation, are present in long-term experimental diabetes. *American Journal of Physiology. Heart and Circulatory Physiology*, *297*(6), H2109–H2119. https://doi.org/10.1152/ajpheart.00157.2009

Asbun, J., & Villarreal, F. J. (2006). The pathogenesis of myocardial fibrosis in the setting of diabetic cardiomyopathy. *Journal of the American College of Cardiology*, *47*, 693–700. https://doi.org/10.1016/j.jacc.2005.09.050

Basu, R., Oudit, G. Y., Wang, X., Zhang, L., Ussher, J. R., Lopaschuk, G. D., & Kassiri, Z. (2009). Type 1 diabetic cardiomyopathy in the Akita (Ins2WT/C96Y) mouse model is characterized by lipotoxicity and diastolic dysfunction with preserved systolic function. *American Journal of Physiology. Heart and Circulatory Physiology*, *297*, H2096–H2108. https://doi.org/10.1152/ajpheart.00452.2009

Blanc, F. X., Coirault, C., Salmeron, S., Chemla, D., & Le Carpentier, Y. (2003). Mechanics and crossbridge kinetics of tracheal smooth muscle in two inbred rat strain. *European Respiratory Journal*, *22*, 227–234. https://doi.org/10.1183/09031936.03.00064203

Brown, R. A., Anthony, M. J., Petrovski, P., & Ren, J. (2001). The influence of gender, diabetes, and acetaldehyde on the intrinsic contractile properties of isolated rat myocardium. *Cardiovascular Toxicology*, *1*, 35–42. https://doi.org/10.1385/CT:1:1:35

Brunello, E., Fusi, L., Ghisleni, A., Park-Holohan, S., Ovejero, J. G., Narayanan, T., & Irving, M. (2020). Myosin filament-based regulation of the dynamics of contraction in heart muscle. *Proceedings of the National Academy of Sciences, USA*, *117*(14), 8177–8186. https://doi.org/10.1073/pnas.1920632117

Bupha-Intr, T., Oo, Y. W., & Wattanapermpool, J. (2011). Increased myocardial stiffness with maintenance of length-dependent calcium activation by female sex hormones in diabetic rats. *American Journal of Physiology. Heart and Circulatory Physiology*, *300*, H1661–H1668. https://doi.org/10.1152/ajpheart.00411.2010

Chattou, S., Diacono, J., & Feuvray, D. (1999). Decrease in sodium-calcium exchange and calcium currents in diabetic rat ventricular myocytes. *Acta Physiologica Scandinavica*, *166*(2), 137–144. https://doi.org/10.1046/j.1365-201x.1999.00547.x

Coirault, C., Chemla, D., Péry-Man, N., Suard, I., & Le Carpentier, Y. (1995). Effects of fatigue on tension-velocity relation of diaphragm. Energetic implication. *American Journal of Respiratory and Critical Care Medicine*, *151*, 123–128. https://doi.org/10.1164/ajrccm.151.1.7812541

Dhalla, N. S., Liu, X., Panagia, V., & Takeda, N. (1998). Subcellular remodeling and heart dysfunction in chronic diabetes. *Cardiovascular Research*, *40*, 239–247. https://doi.org/10.1016/S0008-6363(98)00186-2

Dillmann, W. H. (1980). Diabetes mellitus induces changes in cardiac myosin of the rat. *Diabetes*, *29*, 579–582. https://doi.org/10.2337/diab.29.7.579

Eisenberg, E., Hil, L. T. L., & Chen, Y. D. (1980). Cross-bridge model of muscle contraction: quantitative analysis. *Biophysical Journal*, *29*, 195–227. https://doi.org/10.1016/S0006-3495(80)85126-5

Falcão-Pires, I., & Leite-Moreira, A. F. (2012). Diabetic cardiomyopathy: understanding the molecular and cellular basis to progress in diagnosis and treatment. *Heart Failure Reviews*, *17*, 325–344. https://doi.org/10.1007/s10741-011-9257-z

Fein, F. S., Kornstein, L. B., Strobeck, J. E., Capasso, J. M., & Sonnenblick, E. H. (1980). Altered myocardial mechanics in diabetic rats. *Circulation Research*, *47*, 922–933. https://doi.org/10.1161/01.RES.47.6.922

Fein, F. S., & Sonnenblick, E. H. (1994). Diabetic cardiomyopathy. *Cardiovascular Drugs and Therapy*, *8*, 65–73. https://doi.org/10.1007/BF00877091

Fenwick, A. J., Awinda, P. O., Yarbrough-Jones, J. A., Eldridge, J. A., Rodgers, B. D., & Tanner, B. C. W. (2019). Demembranated skeletal and cardiac fibers produce less force with altered cross-bridge kinetics in a mouse model for limb-girdle muscular dystrophy 2i. *American Journal of Physiology. Cell Physiology*, *317*(2), C226–C234. https://doi.org/10.1152/ajpcell.00524.2018

Flagg, T. P., Cazorla, O., Remedi, M. S., Haim, T. E., Tones, M. A., Bahinski, A., Numann, R. E., Kovacs, A., Schaffer, J. E., Nichols, C. G., & Nerbonne, J. M. (2009). Ca^{2+}-independent alterations in diastolic sarcomere length and relaxation kinetics in a mouse model of lipotoxic diabetic cardiomyopathy. *Circulation Research*, *104*, 95–103. https://doi.org/10.1161/CIRCRESAHA.108.186809

Grundy, D. (2015). Principles and standards for reporting animal experiments in *The Journal of Physiology* and *Experimental Physiology*. *Experimental Physiology* *100*(7), 755–758. https://doi.org/10.1113/EP085299

Guariguata, L., Whiting, D. R., Hambleton, I., Beagley, J., Linnenkamp, U., & Shaw, J. E. (2014). Global estimates of diabetes prevalence for 2013 and projections for 2035. *Diabetes Research and Clinical Practice*, *103*, 137–149. https://doi.org/10.1016/j.diabres.2013.11.002

Han, J. C., Tran, K., Nielsen, P. M., Taberner, A. J., & Loiselle, D. S. (2014). Streptozotocin-induced diabetes prolongs twitch duration without affecting the energetics of isolated ventricular trabeculae. *Cardiovascular Diabetology*, *13*, 79–94. https://doi.org/10.1186/1475-2840-13-79

Hattori, Y., Matsuda, N., Kimura, J., Ishitani, T., Tamada, A., Gando, S., & Kanno, M. (2000). Diminished function and expression of the cardiac Na^{+}-Ca^{2+} exchanger in diabetic rats: implication in Ca^{2+} overload. *Journal of Physiology*, *527*, 85–94. https://doi.org/10.1111/j.1469-7793.2000.00085.x

Henning, R. J. (2020), Diagnosis and treatment of heart failure with preserved left ventricular ejection fraction. *World Journal of Cardiology*, *12*(1), 7–25.

Hill, A. V. (1964). The efficiency of mechanical power development during muscular shortening and its relation to load. *Proceedings of the Royal Society of London. Series B, Biological sciences*, *159*, 319–324.

Howarth, F. C., Quareshi, M. A., Lawrence, P., & Adeghate, E. (2000). Chronic effects of streptozotocin-induced diabetes on the ultrastructure of rat ventricular and papillary muscle. *Acta Diabetologica*, *37*(3), 119–124. https://doi.org/10.1007/s005920070013

Huxley, A. F., & Simmons, R. M. (1971a). Mechanical properties of the cross-bridges of frog striated muscle. *Journal of Physiology*, *218*(Suppl), 59P–60P.

Huxley, A. F., & Simmons, R. M. (1971b). Proposed mechanism of force generation in striated muscle. *Nature*, *233*, 533–538. https://doi.org/10.1038/233533a0

Huynh, T., Harty, B. J., Claggett, B., Fleg, J. L., McKinlay, S. M., Anand, I. S., Lewis, E. F., Joseph, J., Desai, A. S., Sweitzer, N. K., O'Meara, E., Pitt, B., Pfeffer, M. A., & Rouleau, J. L. (2019). Comparison of outcomes in patients with diabetes mellitus treated with versus without insulin + heart failure with preserved left ventricular ejection fraction (from the TOPCAT Study). *American Journal of Cardiology*, *123*, 611–617. https://doi.org/10.1016/j.amjcard.2018.11.022

Isola, M., Ekström, J., Diana, M., Solinas, P., Cossu, M., Lilliu, M. A., Loy, F., & Isola, R. (2013). Subcellular distribution of melatonin receptors in human parotid glands. *Journal of Anatomy*, *223*(5), 519–524. https://doi.org/10.1111/joa.12105

Joseph, T., Coirault, C., Dubourg, O., & Lecarpentier, Y. (2005). Changes in crossbridge mechanical properties in diabetic rat cardiomyopathy. *Basic Research in Cardiology*, *100*(3), 231–239. https://doi.org/10.1007/s00395-005-0512-5

Kampourakis, T., & Irving, M. (2015). Phosphorylation of myosin regulatory light chain controls myosin head conformation in cardiac muscle. *Journal*

of Molecular and Cellular Cardiology, *85*, 199–206. https://doi.org/10.1016/j.yjmcc.2015.06.002

Kita, Y., Shimizu, M., Sugihara, N., Shimizu, K., Yoshio, H., Shibayama, S., & Takeda, R. (1991). Correlation between histopathological changes and mechanical dysfunction in diabetic rat hearts. *Diabetes Research and Clinical Practice*, *11*(3), 177–188. https://doi.org/10.1016/S0168-8227(05)80031-2

Krenz, M., & Robbins, J. (2004). Impact of beta-myosin heavy chain expression on cardiac function during stress. *Journal of the American College of Cardiology*, *44*, 2390–2397. https://doi.org/10.1016/j.jacc.2004.09.044

Krüger, M., Babicz, K., von Frieling-Salewsky, M., & Linke, W. A. (2010). Insulin signaling regulates cardiac titin properties in heart development and diabetic cardiomyopathy. *Journal of Molecular and Cellular Cardiology*, *48*(5), 910–916. https://doi.org/10.1016/j.yjmcc.2010.02.012

Lacombe, V. A., Viatchenko-Karpinski, S., Terentyev, D., Sridhar, A., Emani, S., Bonagura, J. D., & Carnes, C. A. (2007). Mechanisms of impaired calcium handling underlying subclinical diastolic dysfunction in diabetes. *American Journal of Physiology. Regulatory, Integrative and Comparative Physiology*, *293*, R1787–R1797. https://doi.org/10.1152/ajpregu.00059.2007

Lecarpentier, Y., Bugaisky, L. B., Chemla, D., Mercadier, J. J., Schwartz, K., Whalen, R. G., & Martin, J. L. (1987). Coordinated changes in contractility, energetics, and isomyosins after aortic stenosis. *American Journal of Physiology*, *252*, H275–H282.

Lecarpentier, Y., Chemla, D., Blanc, F. X., Pourny, J. C., Joseph, T., Riou, B., & Coirault, C. (1998). Mechanics, energetics and crossbridge kinetics of rabbit diaphragm during congestive heart failure. *FASEB Journal*, *12*, 981–989. https://doi.org/10.1096/fasebj.12.11.981

Lee, S. I., Patel, M., Jones, C. M., & Narendran, P. (2015). Cardiovascular disease and type 1 diabetes: prevalence, prediction and management in an ageing population. *Therapeutic Advances in Chronic Disease*, *6*, 347–374. https://doi.org/10.1177/2040622315598502

Lindman, B. R. (2017). The diabetic heart failure with preserved ejection fraction phenotype. Is it real and is it worth targeting therapeutically? *Circulation*, *135*, 736–740. https://doi.org/10.1161/CIRCULATIONAHA.116.025957

Litwin, S. E., Raya, T. E., Anderson, P. G., Daugherty, S., & Goldman, S. (1990). Abnormal cardiac function in the streptozotocin-diabetic rat. Changes in active and passive properties of the left ventricle. *Journal of Clinical Investigation*, *86*, 481–488. https://doi.org/10.1172/JCI114734

Liu, X., Takeda, N., & Dhalla, N. S. (1997). Myosin light-chain phosphorylation in diabetic cardiomyopathy in rats. *Metabolism*, *46*(1), 71–75. https://doi.org/10.1016/S0026-0495(97)90171-2

Locher, M.R., Razumova, M.V., Stelzer, J.E., Norman, H.S., Patel, J.R., & Moss, R.L. (2009). Determination of rate constants for turnover of myosin isoforms in rat myocardium: implications for in vivo contractile kinetics. *Am J Physiol Heart Circ Physiol*, *297*(1), 247–256. https://doi.org/10.1152/ajpheart.00922.2008.

Loy, F., Isola, M., Isola, R., Lilliu, M. A., Solinas, P., Conti, G., Godoy, T., Riva, A., & Ekström, J. (2014). The antipsychotic amisulpride: ultrastructural evidence of its secretory activity in salivary glands. *Oral Diseases*, *20*(8), 796–802.

Malhotra, A., & Sanghi, V. (1997). Regulation of contractile proteins in diabetic heart. *Cardiovascular Research*, *34*, 34–40. https://doi.org/10.1016/S0008-6363(97)00059-X

Malmqvist, U. P., Aronshtam, A., & Lowey, S. (2004). Cardiac myosin isoforms from different species have unique enzymatic and mechanical properties. *Biochemistry*, *43*(47), 15058–15065. https://doi.org/10.1021/bi0495329

Mancinelli, R., Vargiu, R., Cappa, i A., Floris, G., Fraschini, M., & Faa, G. (2005). A metabolic approach to the treatment of dilated cardiomyopathy in BIO T0-2 cardiomyopathic Syrian hamsters. *Biofactors*, *25*, 127–135. https://doi.org/10.1002/biof.5520250114

Nemoto, O., Kawaguchi, M., Yaoita, H., Miyake, K., Maehara, K., & Maruyama, Y. (2006). Left ventricular dysfunction and remodeling in streptozotocin-induced diabetic rats. *Circulation Journal*, *70*, 327–334. https://doi.org/10.1253/circj.70.327

Norby, F. L., Aberle, N. S., Kajstura, J., Anversa, P., & Ren, J. (2004). Transgenic overexpression of insulin-like growth factor I prevents streptozotocin-induced cardiac contractile dysfunction and beta-adrenergic response in ventricular myocytes. *Journal of Endocrinology*, *180*, 175–182. https://doi.org/10.1677/joe.0.1800175

Palmiter, K. A., Tyska, M. J., Dupuis, D. E., Alpert, N. R., & Warshaw, D. M. (1999). Kinetic differences at the single molecule level account for the functional diversity of rabbit cardiac myosin isoforms. *Journal of Physiology*, *519*(3), 669–678. https://doi.org/10.1111/j.1469-7793.1999.0669n.x

Paradise, N. F., Schmitter, J. L., & Surmitis, J. M. (1981). Criteria for adequate oxygenation of isometric kitten papillary muscle. *American Journal of Physiology*, *241*, H348–H353.

Regitz-Zagrosek, V., & Kararigas, G. (2017). Mechanistic pathways of sex differences in cardiovascular disease. *Physiological Reviews*, *97*(1), 1–37. https://doi.org/10.1152/physrev.00021.2015

Ren, J., & Bode, A. M. (2000). Altered cardiac exicitation-contraction coupling in ventricular myocytes from spontaneously diabetic BB rats. *American Journal of Physiology. Heart and Circulatory Physiology*, *279*, H238–H244. https://doi.org/10.1152/ajpheart.2000.279.1.H238

Riva, A., Tandler, B., Ushiki, T., Usai, P., Isola, R., Conti, G., Loy, F., & Hoppel, C. L. (2011). Mitochondria of human Leydig cells as seen by high resolution scanning electron microscopy. *Archives of Histology and Cytology*, *73*(1), 37–44. https://doi.org/10.1679/aohc.73.37

Schmid, M., & Toepfer, C. N. (2021). Cardiac myosin super relaxation (SRX): a perspective on fundamental biology, human disease and therapeutics. *Biology Open*, *10*, bio057646. https://doi.org/10.1242/bio.057646 PMID: 33589442

Siri, F. M., Malhotra, A., Factor, S. M., Sonnenblick, E. H., & Fein, F. S. (1997). Prolonged ejection duration helps to maintain pump performance of the renal-hypertensive-diabetic rat heart: correlations between isolated papillary muscle function and ventricular performance in situ. *Cardiovascular Research*, *34*, 230–240. https://doi.org/10.1016/S0008-6363(96)00239-8

Sowers, J. R. (1998). Diabetes mellitus and cardiovascular disease in women. *Archives of Internal Medicine*, *158*, 617–621. https://doi.org/10.1001/archinte.158.6.617

Sugiura, S., Kobayakawa, N., Momomura, S., Chaen, S., Omata, M., & Sugi, H. (1996). Different cardiac myosin isoforms exhibit equal force-generating ability in vitro. *Biochimica et Biophysica Acta*, *1273*(2), 73–76. https://doi.org/10.1016/0005-2728(95)00149-2

Takeda, Y., Sakata, Y., Mano, T., Ohtani, T., Kamimura, D., Tamaki, S., Omori, Y., Tsukamoto, Y., Aizawa, Y., Komuro, I., & Yamamoto, K. (2011). Competing risks of heart failure with preserved ejection fraction in diabetic patients. *European Journal of Heart Failure*, *13*, 664–669. https://doi.org/10.1093/eurjhf/hfr019

Thompson, E. W. (1994). Quantitative analysis of myocardial structure in insulin-dependent diabetes mellitus: effects of immediate and delayed insulin replacement. *Proceedings of the Society for Experimental Biology and Medicine*, *205*, 294–305. https://doi.org/10.3181/00379727-205-43710

Trost, S. U., Belke, D. D., Bluhm, W. F., Meyer, M., Swanson, E., & Dillmann, W. H. (2002). Overexpression of the sarcoplasmic reticulum Ca^{2+}-ATPase improves myocardial contractility in diabetic cardiomyopathy. *Diabetes*, *51*, 1166–1171. https://doi.org/10.2337/diabetes.51.4.1166

van der Velden, J., & Stienen, G. J. M. (2019). Cardiac disorders and pathophysiology of sarcomeric proteins. *Physiological Reviews*, *99*(1), 381–426. https://doi.org/10.1152/physrev.00040.2017

van Heerebeek, L., Hamdani, N., Handoko, M. L., Falcao-Pires, I., Musters, R. J., Kupreishvili, K., Ijsselmuiden, A. J. J., Schalkwijk, C. G., Bronzwaer, J. G.

F., Diamant, M., Borbély, A., van der Velden, J., Stienen, G. J. M., Laarman, G. J., Niessen, H. W. M., & Paulus, W. J. (2008). Diastolic stiffness of the failing diabetic heart: importance of fibrosis, advanced glycation end products, and myocyte resting tension. *Circulation*, *117*, 43–51. https://doi.org/10.1161/CIRCULATIONAHA.107.728550

Vargiu, R., Littarru, G. P., Fraschini, M., Perinu, A., Tiano, L., Capra, A., & Mancinelli, R. (2010). Enhancement of shortening velocity, power, and acto-myosin cross bridge (CB) kinetics following long-term treatment with propionyl-L-carnitine, coenzyme Q_{10} and omega-3 fatty acids in BIO T0-2 cardiomyopathic Syrian Hamsters papillary muscle. *Biofactors*, *36*, 229–239. https://doi.org/10.1002/biof.95

Waddingham, M. T., Edgley, A. J., Tsuchimochi, H., Kelly, D. J., Shirai, M., & Pearson, J. T. (2015). Contractile apparatus dysfunction early in the pathophysiology of diabetic cardiomyopathy. *World Journal of Diabetes*, *6*, 943–960. https://doi.org/10.4239/wjd.v6.i7.943

Woledge, R. C., Curtin, N. A., & Homsher, E. (1985). Energetic aspects of muscle contraction. *Monographs of the Physiological Society*, *41*, 27–117.

Zhang, L., Cannell, M. B., Phillips, A. R. J., Cooper, G. J. S., & War, D. M. L. (2008). Altered calcium homeostasis does not explain the contractile deficit of diabetic cardiomyopathy. *Diabetes*, *57*, 2158–2166. https://doi.org/10.2337/db08-0140

Zhao, S. M., Wang, Y. L., Guo, C. Y., Chen, J. L., & Wu, Y. Q. (2014). Progressive decay of Ca^{2+} homeostasis in the development of diabetic cardiomyopathy. *Cardiovasc Diabetol*, *13*, 75. https://doi.org/10.1186/1475-2840-13-75

Zile, M. R., Baicu, C. F., Ikonomidis, J. S., Stroud, R. E., Nietert, P. J., Bradshaw, A. D., Slater, R., Palmer, B. M., Van Buren, P., Meyer, M., Redfield, M. M., Bull, D. A., Granzier, H. L., & LeWinter, M. M. (2015). Myocardial stiffness in patients with heart failure and a preserved ejection fraction: contributions of collagen and titin. *Circulation*, *131*(14), 1247–1259. https://doi.org/10.1161/CIRCULATIONAHA.114.013215

How to cite this article: Isola, R., Broccia, F., Casti, A., Loy, F., Isola, M., & Vargiu, R. (2021). STZ-diabetic rat heart maintains developed tension amplitude by increasing sarcomere length and crossbridge density. *Experimental Physiology*, 1–15. https://doi.org/10.1113/EP089000